Appl. Phys. B 63, 311–314 (1996)

Applied Physics B Lasers and Optics

Rapid communication

The $C^1\Sigma^+$–$B^1\Sigma^+$ amplified spontaneous emission in CO

H. Hasegawa*, K. Tsukiyama**

Department of Chemistry, Faculty of Science, Science University of Tokyo, Kagurazaka, Shinjuku, Tokyo 162, Japan

Received: 9 April 1996/Accepted: 24 June 1996

Abstract. The first observation of the amplified spontaneous emission (ASE) from the Rydberg $C^1\Sigma^+(v'=0)$ state of CO is reported. When the $C^1\Sigma^+(v'=0)$ state was populated through the two-photon excitation, infrared radiation near 2.0 μm was ejected in forward as well as backward directions along the laser propagation. The assignment as the $C^1\Sigma^+(v'=0) \rightarrow B^1\Sigma^+(v=0)$ transition was confirmed. Several characteristics of ASE from the $C^1\Sigma^+(v'=0)$ state are presented.

PACS: 33.20; 32.80

Amplified Spontaneous Emission (ASE), also termed stimulated emission [1], is a quasicoherent radiation created by an inverted population of atoms and molecules. In recent years, Laser-Induced ASE (LIASE) technique has been applied successfully to the detection of atomic species such as H [2], C [3], N [4] and O [5, 6]. Several investigations on ASE in molecular systems have been reported. Westblom et al. [1] studied two-photon-induced ASE from the $B^1\Sigma^+$ state of CO. Czarnetzki et al. [7] observed near-infrared ASE corresponding to the $EF^1\Sigma_g^+$–$B^1\Sigma_u^+$ transition in two-photon excited H_2. More recently, our group made a thorough investigation on the cascading inter-Rydberg ASE transitions in NO Rydberg states populated through ultraviolet–visible double-resonance excitation [8]. Our work demonstrated a tremendous potential of LIASE as a spectroscopic technique for highly excited levels of small molecules. In this Communication, we wish to describe the characteristics of ASE following the two-photon excitation of CO in the $C^1\Sigma^+(v'=0)$ state. The schematic level diagram for the relevant Rydberg states of CO is illustrated in Fig. 1. The results are to be compared with those of the $B^1\Sigma^+(v=0)$ state [1].

The experiment was performed using a dye laser (Quanta Ray, PDL-2) pumped by a Q-switched YAG laser (Quanta-Ray, DCR-2A). The output of the dye laser (laser dye; C-440 in methanol) was frequency-doubled by a BBO crystal. The UV pulse energy is estimated to be ~ 100 μJ/pulse. The second harmonic was then separated from the fundamental radiation by the use of a Pellin-Broca prism. The scan of the UV frequency was controlled by a home-made autotracker. The UV beam was focused into a quartz cell with a lens ($f = 100$ mm). The IR radiation emitted in the same direction as the laser propagation was collimated with a lens ($f = 80$ mm) after being separated from the pump beam by appropriate optical filters. Several photodiodes were used properly: Electro-Optics Technology ET-4000; 0.35–1.1 μm, Hamamatsu B1720-02; 0.8–1.7 μm; Hamamatsu P2682, 1.0–2.5 μm. A current preamplifier (NF Circuit Design LI-76 or Hamamatsu C3757-02) was employed at need. A 27.5 cm monochromator (Acton Research SP401, 300 grooves/mm blazed at 2 μm) was employed to disperse the IR emission. The polarization of the IR radiation was measured with a Glan laser polarizer. Signals from detectors were averaged by boxcar integrators (Stanford Research SR250) which were interfaced to a personal computer. The ultra-high purity CO was commercially obtained.

Figure 2 illustrates the two-photon excitation spectrum for the total infrared emission in the region of $C^1\Sigma^+(v'=0) \leftarrow\leftarrow X^1\Sigma^+(v''=0)$ transition. Hereafter, we shall indicate quantities associated with $X^1\Sigma^+$ and $C^1\Sigma^+$ states by double ($''$) and single ($'$) prime mark, respectively. The spectrum consists of a broad peak assignable to the Q branch. Because of the nearly identical rotational constants of the $X^1\Sigma^+$ and $C^1\Sigma^+$, the Q branch lines of low J'' values overlap too closely to be resolved. The P and R branches carry no transition moment in the two-photon $^1\Sigma^+$–$^1\Sigma^+$ excitation.

* *Current address*: Department of Pure and Applied Sciences, College of Arts and Sciences, The University of Tokyo, Komaba, Meguro, Tokyo 153 Japan.
** Corresponding author

This work was supported by the Morino Foundation, a Grant-in-Aid (No. 07640697) and that on Priority-Area-Research "Photoreaction Dynamics" (No. 07228268) from the Ministry of Education, Science, Sports and Culture, Japan.

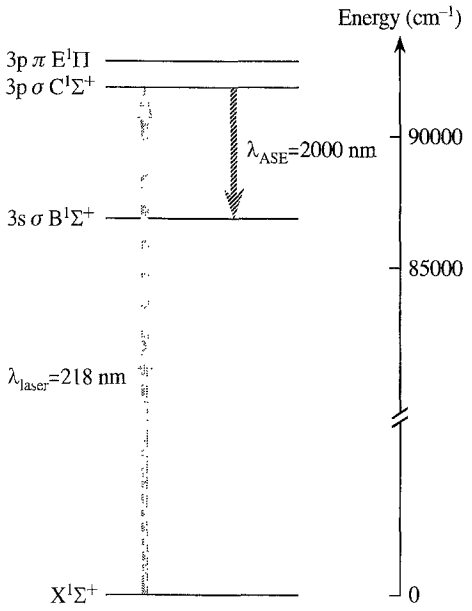

Fig. 1. Simplified energy level scheme of CO, indicating the transitions pertinent to this work

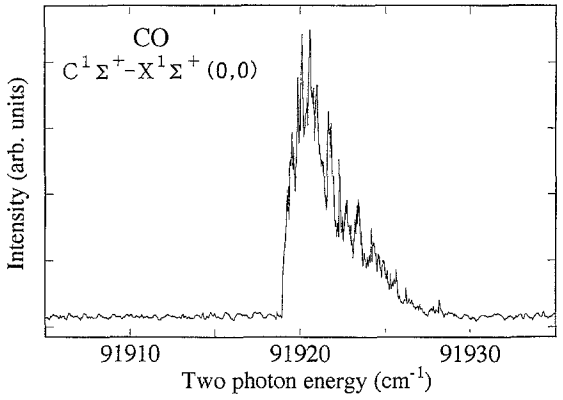

Fig. 2 Two-photon ASE excitation spectrum of CO $C^1\Sigma^+(v'=0) \leftarrow\leftarrow X^1\Sigma^+(v''=0)$ transition; CO pressure: 100 Torr

Figure 3 depicts a typical dispersed IR spectrum where the UV laser frequency was fixed near the broad unresolved peak in Fig. 2. The emission is located around 2.0 μm corresponding to the $C^1\Sigma^+(v'=0) \rightarrow B^1\Sigma^+(v=0)$ transition [9]. The rotational assignment is straightforward; the absolute rotational numbering was unambiguously achieved from the energy difference of the P and R branches. In our previous double-resonant experiment [10] on the four-wave mixing in CO, the lack of convenient frequency standard below 500 nm prevented us from the assignment of rotational quantum numbers (J') in the $C^1\Sigma^+(v'=0)$ state. The detection of two-photon-induced ASE offers a simple and convenient method for the identification of J'.

The spatial pattern of the IR radiation could be estimated by sliding the photodiode detector horizontally without the collimating lens. At a distance of 12 cm from the laser focus, the beam width (FWHM) is ~ 8 mm, indicating that the radiation is highly collimated. The IR

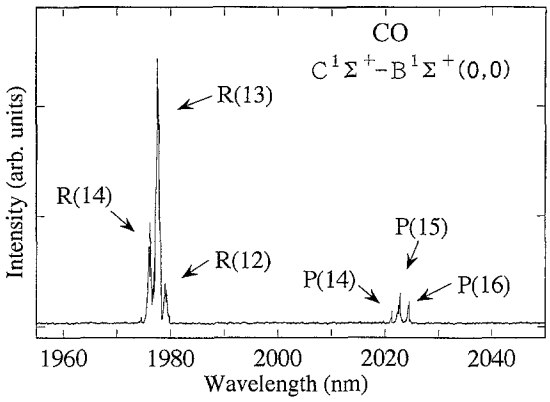

Fig. 3. Typical dispersed ASE spectrum corresponding to the $C^1\Sigma^+(v'=0) \rightarrow B^1\Sigma^+(v=0)$ transition. Numbers in parentheses denote the rotational quantum number of the $B^1\Sigma^+(v=0)$ state; CO pressure: 100 Torr

radiation was generated in forward as well as backward directions along the laser beam. This fact supports vigorously that the observed IR radiation is ASE originating from the inverted population between the $C^1\Sigma^+(v'=0)$ and $B^1\Sigma^+(v=0)$ states. No sign of ASE in the visible region was detectable, implying the $C^1\Sigma^+(v'=0) \rightarrow A^1\Pi(v)$ transition is not a major ASE relaxation pathway. *Ab initio* calculations estimated that the $C^1\Sigma^+ \rightarrow B^1\Sigma^+$ and $C^1\Sigma^+ \rightarrow A^1\Pi$ transition probabilities are fairly similar [11]. On the other hand, the critical population inversion density (n_c) for the threshold condition of ASE amplification is proportional to $1/\lambda^2$ [12], which suggests preferential ASE amplification at longer wavelengths.

Westblom et al. [1] succeeded to observe the $B^1\Sigma^+(v=0) \rightarrow A^1\Pi(v)$ ASE near 500 nm when the $B^1\Sigma^+(v=0)$ state was directly populated through two-photon excitation. We believe that the lack of visible ASE is attributable to the lower laser power used in the present study; their laser pulse energy, ~ 2 mJ/pulse, is more than one magnitude intense than ours. The $B^1\Sigma^+$ population transfered from the $C^1\Sigma^+$ state may be too low to reach the threshold for the $B^1\Sigma^+(v=0) \rightarrow A^1\Pi(v)$ ASE transitions. Under our experimental conditions, the major relaxation process from the $B^1\Sigma^+(v=0)$ state must be collisional deactivation and spontaneous emission to the ground state. ASE transitions from $B^1\Sigma^+(v=0)$ to $X^1\Sigma^+(v'' \geqq 1)$ is unlikely to occur because 1) the $B^1\Sigma^+$ and $X^1\Sigma^+$ potential curves are very similar so that only $\Delta v = 0$ transitions have appreciable Franck–Condon factors and 2) the ASE wavelength falls in the vacuum ultraviolet region.

For cascading ASE processes in NO investigated by our group [8], only the inter-Rydberg ASE transitions have been detected. This observation was partly explained by that the oscillator strengths of the inter-Rydberg transitions are concentrated in the $\Delta v = 0$, whereas the Franck-Condon factors are distributed for a large range of Δv in the Rydberg-valence transition. The similar interpretation applies successfully to the ASE process in CO; both $B^1\Sigma^+(3s\sigma)$ and $C^1\Sigma^+(3p\sigma)$ states belong to the lowest Rydberg member, while the $A^1\Pi$ state has a valence character.

It is known that two-photon excitation can induce parametric four-wave mixing (PFWM) in several atomic [13, 14] and molecular [7] systems; when a non-linear medium absorbs two photons of frequency ω_1, a pair of photons with frequencies ω_2 and ω_3 are generated satisfying energy conservation ($2\omega_1 = \omega_2 + \omega_3$) as well as the phase-matching condition. It was proposed that the forward-emitted ASE couples with the two-photon pump beam producing a four-wave mixed signal at a resonance line. In the present case, PFWM might generate coherent 115 nm radiation corresponding to the $B^1\Sigma^+(v=0)$–$X^1\Sigma^+(v''=0)$ energy difference [15]. An attempt to detect this VUV radiation in the separate system was unsuccessful. The presence of backward signal argues against significant contribution from PFWM which is only phase-matched in the forward direction. Apparently, the IR radiation is not polarized as shown in Fig. 4, which would mean the incoherent nature of the ASE process. Unpolarized character of ASE has been reported recently [8, 16]. Under our experimental conditions, we have no positive evidence for the occurence of PFWM process in CO.

As seen in Fig. 3, the intensity of the R branch in high J region is much stronger than that of the P branch. On the contrary, the P branch is dominant for $J' < 5$. It is interesting to quote the fluorescence emission (FE) spectrum of $^{12}C^{18}O$ in a discharge (Fig. 1 in [9]); the intensity ratio of the R to P branch slightly exceeds 1 for $J' > 9$, is nearly unity for J' around 8, and is below 1 for $J' < 6$. The inversion of the R/P ratio around $J' = 8$ is common to both ASE and FE spectra. In the former, however, the contrast between stronger and weaker transitions is apparently displayed in an exaggerated fashion. Similar characteristic, that is, intense peaks in the fluorescence spectrum are emphasized in the ASE spectrum, was also seen in the $B^1\Sigma^+(v=0) \rightarrow A^1\Pi(v)$ transitions [1]: ASE occurs in only a few vibronic transitions with the largest Franck-Condon factors, while the fluorescence emission exhibits a smooth Franck-Condon parabola.

An attempt to observe ASE from the $E^1\Pi(3p\pi)(v=0)$ state [17] located just above the $C^1\Sigma^+(v'=0)$ state failed. No trace of ASE around 1.66 μm [18] corresponding to the $E^1\Pi(v=0) \rightarrow B^1\Sigma^+(v=0)$ transition was detectable. This might be due to the weak predissociative character of the $E^1\Pi(v=0)$ state [19] which immediately reduces the inverted population density below the threshold; predissociation is favored over fluorescence by a factor of 9 [20].

Figure 5a shows total ASE signal strengths as a function of CO pressure in the cell. Figure 5b illustrates the partially resolved R branch at different pressures. Although the spectral resolution is not as good as Fig. 3, it is obvious that the overall pattern does not change considerably with pressure. In other words, collisionally populated nearby rotational levels contribute little to the ASE process. In the ASE of the $B^1\Sigma^+(v=0)$ state, the collisionally transfered triplet system ($b^3\Sigma^+ \rightarrow a^3\Pi$) appears in the fluorescence spectrum but does not in the ASE spectrum [1]. At higher pressures, collisions distribute the $C^1\Sigma^+$ population among rotational levels within the laser pulse duration, resulting in the distribution of the ASE gain among many rovibronic transitions. Consequently, the non-linear nature of the gain process would cause the total gain to diminish rapidly, which might be one of the factors for the rapid decrease of the ASE intensity as shown in Fig. 5a.

The two-photon $^1\Sigma^+$–$^1\Sigma^+$ bands in CO, $B^1\Sigma^+(v=0) \leftarrow \leftarrow$ as well as $C^1\Sigma^+(v'=0) \leftarrow \leftarrow X^1\Sigma^+(v''=0)$, have been served as model transitions for the feasibility of

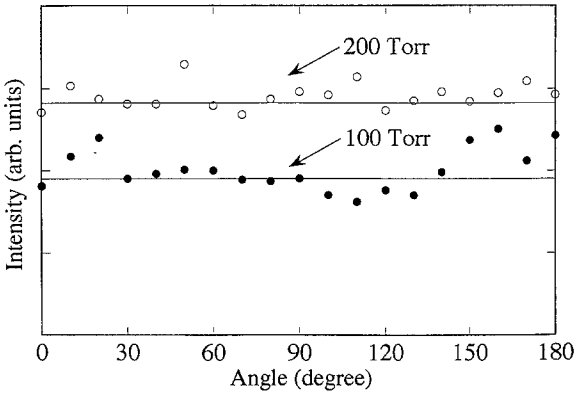

Fig. 4. Total ASE intensity vs rotation angle of the Glan laser polarizer. Laser frequency was fixed near the peak ($J' \sim 10$) of the excitation spectrum at 200 Torr and at slightly blue side ($J' \sim 15$) of the peak at 100 Torr

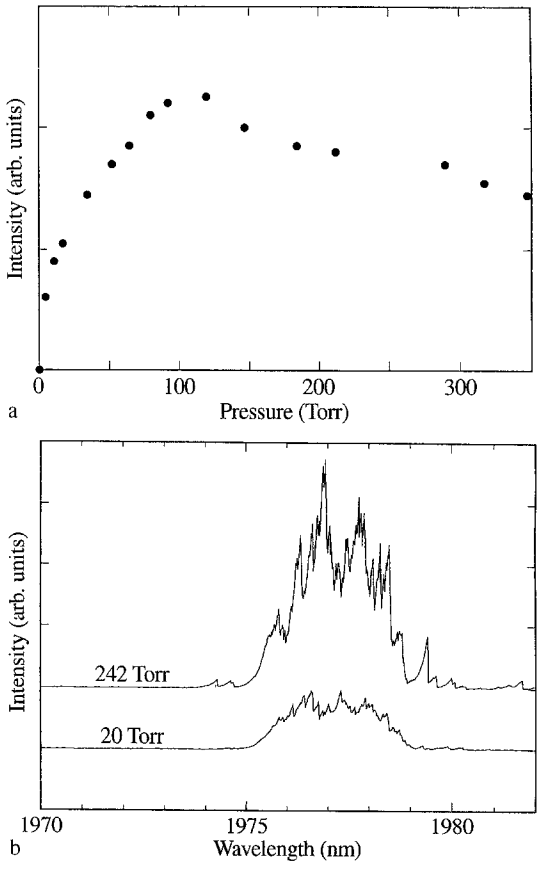

Fig. 5. **a** Total ASE intensity vs CO pressure. Laser frequency was fixed near the peak ($J' \sim 10$) of the excitation spectrum; **b** The effect of pressure on the spectral pattern of the R branch of the $C^1\Sigma^+ \rightarrow B^1\Sigma^+(0,0)$ transition. The $R(13)$, $R(14)$ and $R(15)$ lines are partially resolved

various laser spectroscopic techniques such as resonance-enhanced multiphoton ionization (REMPI) [21], two-photon-induced polarization (TIP) [22] and degenerate four-wave mixing (DFWM) [23]. The distinct advantage of the present method is that the signal wave is generated in the infrared region with a narrow solid angle. Accordingly, a simple optical filtering can separate the signal beam from the intense laser radiation perfectly. The generation of a signal wave in backward as well as forward directions may be useful for the application that provides with optical approach in only one way.

References

1. U. Westblom, S. Agrup, M. Alden, H.M. Hertz, J.E.M. Goldsmith: Appl. Phys. **B50**, 487 (1990)
2. J.M.E. Goldsmith: J. Opt. Soc. Am. **B6**, 1979 (1989)
3. M.A. Alden, P.-E. Bengtsson, U. Westblom: Opt. Commun. **71**, 263 (1989)
4. S. Agrup, U. Westblom, M. Alden: Chem. Phys. Lett. **170**, 406 (1990)
5. M. Alden, U. Westblom, J.E.M. Goldsmith: Opt. Lett. **14**, 305 (1989)
6. Y-L. Huang, R.J. Gordon: J. Chem. Phys. **97**, 6363 (1992)
7. U. Czarnetzki, H.F. Döbele: Phys. Rev. **A44**, 7530 (1991)
8. J. Ishii, K. Uehara, K. Tsukiyama: J. Chem. Phys. **104**, 499 (1996)
9. J-Y. Roncin, A. Ross, E. Boursey: J. Mol. Spectrosc. **162**, 353 (1993)
10. K. Tsukiyama, M. Tsukakoshi, T. Kasuya: Appl. Phys. **B50**, 23 (1990)
11. K. Kirby, D.L. Cooper: J. Chem. Phys. **90**, 4895 (1989)
12. G.I. Peters, L. Allen: J. Phys. **A4**, 238 (1971)
13. J. Bokor, R.R. Freeman, R.L. Panock, J.C. White: Opt. Lett. **6**, 182 (1981)
14. F.S. Tomkins, R. Mahon: Opt. Lett. **6**, 179 (1981)
15. M. Eidelsberg, J-Y. Roncin, A. Le Floch, F. Launay, C. Letzelter, J. Rostas: J. Mol. Spectrosc. **121**, 309 (1987)
16. N. Omenetto, O.I. Matveev, W. Resto, R. Badini, B.W. Smith, J.D. Winefordner: Appl. Phys. **B58**, 303 (1994)
17. M.A. Hines, H.A. Michelsen, R.N. Zare: J. Chem. Phys. **93**, 8557 (1990)
18. C. Amiot, J-Y. Roncin, J. Verges: J. Phys. **B19**, L19 (1986)
19. P. Cacciani, W. Hogervorst, W. Ubachs: J. Chem. Phys. **102**, 8308 (1995)
20. C. Letzelter, M. Eidelsberg, F. Rostas, J. Breton, B. Thiblemont: Chem. Phys. **114**, 273 (1987)
21. W. Ubachs, P.C. Hinnen, P. Hansen, S. Stolte, W. Hogervorst, P. Cacciani: J. Mol. Spectrosc. **174**, 388 (1995)
22. K. Nyholm, R. Rritzon, N. Georgiev, M. Alden: Opt. Commun. **114**, 76 (1995)
23. N. Georgiev, U. Westblom, M. Alden: Opt. Commun. **94**, 99 (1992)